

REMOVAL OF METHYLENE BLUE FROM AQUEOUS SOLUTIONS USING AN ORDERED MESOPOROUS SiO₂-CaO CERAMIC SORBENT

BACIU D.¹, IOANNOU Z.², STERIOTIS TH.¹, CHARALAMBOPOULOU G.¹ and STUBOS A.¹

¹National Center for Scientific Research "Demokritos", 15310 Agia Paraskevi Attikis, Athens, Greece, ²University of the Aegean, 81400, Metropolitae loakeim 2, Myrina Limnos, Greece
E-mail: zioan@teemail.gr

ABSTRACT

An ordered mesoporous binary ceramic system (SiO₂-CaO) has been successfully synthesized through a hydrothermal method by using polyethylene glycol and cetyltrimethylammonium bromide, as non-ionic co-surfactant and cationic surfactant, respectively. The pertinent structural, morphological and textural properties were investigated by FTIR, XRD, SEM and N₂ adsorption at 77K. SEM results showed that calcination at 600 °C leads to the formation of porous spheres with diameter between 300–400 nm. The obtained material exhibits an ordered mesoporous structure with certain uniformity in pore size and morphology, while it has a mean pore size ca. 4.8 nm, total pore volume of 0.169 cm³/g and BET specific surface area of 134 m²/g. The kinetic analysis of methylene blue (MB) adsorption onto the binary system was studied at three different ratios of adsorbent to MB solution (0.5, 1.5 and 3 g/L) and showed that the binary system adsorbs at least 96% of MB in less than 10 min at a ratio of adsorbent to MB solution equal to 3 g/L. Pseudo-second order is the sole mechanism that describes MB adsorption onto SiO₂-CaO. The equilibrium data analysis showed that Freundlich model describes better MB adsorption onto the new mesoporous SiO₂-CaO material, which depicted a maximum methylene blue adsorption capacity 165.65 µmolg⁻¹ at 23.5 °C.

Keywords: methylene blue dye, adsorption, kinetics, ordered mesoporous binary ceramic materials

1. Introduction

Water contamination caused by a wide range of industries using dyes is an ever-growing problem worldwide, due to the health and environmental hazards associated with such compounds (Fu *et al.*, 2015).

Among azo dyes, methylene blue (MB: CH₃)₂N(C₆H₃)NS⁺(C₆H₃)N(CH₃)₂Cl⁻) is perhaps the most commonly used in industries such as textile, paper, leather, pulp mills, food and plastics, with a severe though environmental pollution impact. As soon as MB enters aquatic ecosystems it can lead to a series of hazards such as human / aquatic animals eye burn, irritation to the gastrointestinal, methemoglobinemia, cyanosis, convulsions, tachycardia, dyspnea, irritation to the skin etc. (Ghaedia *et al.*, 2015; Xiao *et al.*, 2015). Therefore, removal of methylene blue by an ecological and efficient method becomes urgent and pertinent research efforts have attracted significant interest worldwide.

Adsorption is being considered as an economic, effective method to remove pollutants because of its significant advantages, e.g., low cost, ease of operation, variability of possible adsorbents with high resistance towards toxic chemical compounds in water etc. (Fu *et al.*, 2015; Wang *et al.*, 2015). Suitable adsorbents, comprising the core of the adsorption technique, should be highly efficient, stable, low-cost, non-toxic and environmentally compatible (Wang *et al.*, 2015). The removal capacity of an adsorbent mainly depends on its surface properties including surface area and surface ion exchange sites (Xiao *et al.*, 2015). In this respect materials such as activated carbons, zeolite, fly ash, graphene oxide and nanoporous silica are mainly used for the removal of synthetic dyes (Zarezadeh-Mehrzi and Badiei, 2014).

Ordered mesoporous materials, comprising a rather new class of materials (Zhao *et al.*, 1996) possessing rather high surface area, and large pore volume, appear as promising sorbents for a wide range of applications in oil refining, petrochemistry, organic synthesis, waste treatment, and even drug delivery and tissue regeneration (Xiao *et al.*, 2015; Salonen *et al.*, 2005; Yang *et al.*, 2005; Vallet-Regi *et al.*, 2005; Yan *et al.*, 2005).

In the present work, we propose the development of a novel type of adsorbent and its use for MB removal. Specifically, an ordered mesoporous binary ceramic system ($\text{SiO}_2\text{-CaO}$) has been successfully synthesized through a hydrothermal method by using for the first time (to the best of our knowledge) a combination of cetyltrimethylammonium bromide (CTAB) and polyethylene glycol (PEG) as cationic surfactant and non-ionic co-surfactant, respectively. The kinetic analysis of MB adsorption onto the binary system was studied at three different ratios of adsorbent to MB solution (0.5, 1.5 and 3 g/L). Four different kinetic models were used, i.e. pseudo-first order, pseudo-second order, Elovich equation and intraparticle diffusion model. MB adsorption measurements showed that the binary system adsorbs at least 96% of MB in less than 10 min at a ratio of adsorbent to MB solution equal to 3 g/L. Pseudo-second order is the sole mechanism that describes MB adsorption onto $\text{SiO}_2\text{-CaO}$. Furthermore the equilibrium data were fitted using Langmuir and Freundlich adsorption isotherms showing that Freundlich model describes better MB adsorption onto $\text{SiO}_2\text{-CaO}$.

2. Materials & methods

2.1. Preparation of binary ceramic system ($\text{SiO}_2\text{-CaO}$)

The formation process of the binary ceramic system ($\text{SiO}_2\text{-CaO}$) is illustrated in Figure 1. Briefly, 1.0g of PEG particles (Aldrich, average Mn (10.000)) and 0.46g sodium hydrate (Mallinckrodt) were dissolved in 120mL distilled H_2O under vigorous stirring, followed by the addition of 1.40 g of CTAB (Sigma). After stirring for 1 h at room temperature, 1.64 g of $\text{Ca}(\text{NO}_3)_2 \cdot 4\text{H}_2\text{O}$ (Sigma Aldrich) and 5.22 g (5.59 ml) of tetraethyl orthosilicate (Aldrich) were added under vigorous stirring.

The mixture was stirred at room temperature for 24 h and then transferred to Teflon-lined autoclaves. The autoclaves were sealed and heated at 80 °C for 23 h, at 90 °C for 6 h and at 80 °C for 19 h and then allowed to cool down to room temperature naturally. The products were collected by filtration and washed several times with distilled H_2O and ethanol, and dried at 100 °C overnight. Finally, the white powder obtained was calcined in air at 600 °C for 5 h with a heating rate of 9 °C/min.

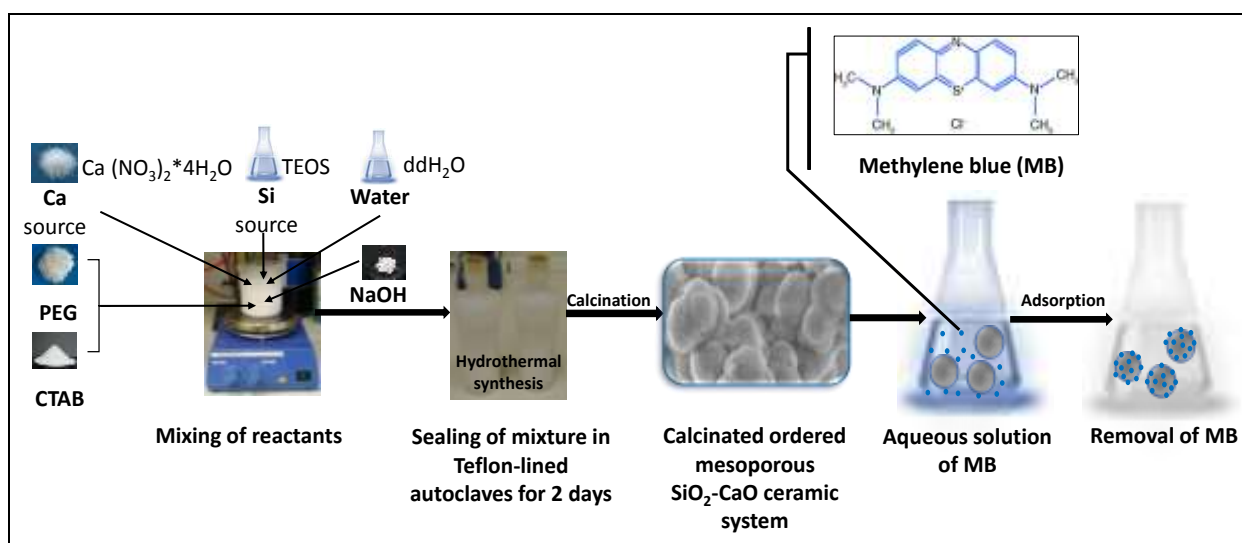


Figure 1: Illustration of the formation process of the binary ($\text{SiO}_2\text{-CaO}$) ceramic system and MB uptake

2.2. Methylene blue adsorption study

An aqueous MB solution with a concentration of 0.0328 g L⁻¹ at 20°C was prepared. An amount of the mesoporous (SiO₂-CaO) adsorbent was placed in 100mL-plastic tubes in an adsorbent – to – MB solution ratio equal to 0.5, 1.0, 1.5, 3.0 g L⁻¹ under continuous stirring. At specific time intervals, an amount of the solution was centrifuged for 5 min at 10,000 rpm and the respective MB concentration was determined by using a Unicam helios gamma UV-VIS spectrophotometer at 664nm. The kinetic experiments were repeated twice. The adsorbed amount (X_t) of MB was deduced from the difference between the initial amount of adsorbate (X₀) in the solution and the measured amount of the adsorbate in every solution sample. pH values were measured for adsorbent to adsorbate solution ratio equal to 0.5, 1.5 and 3 g L⁻¹. The influence of temperature, i.e. 23.5, 50, 70°C, for adsorbent to adsorbate solution ratio equal to 1.5 g L⁻¹ was also studied.

2.3. Characterization of binary ceramic system (SiO₂-CaO)

The powder X-ray diffraction (PXRD) patterns of the samples were recorded on a Rigaku R-AXIS IV Imaging Plate Detector mounted on a Rigaku RU-H3R Rotating Copper Anode X-ray Generator (λ = 1.54 Å).

SEM images of the developed materials were obtained using a Jeol JSM 7401F Field Emission Scanning Electron Microscope (SEM). The materials were subjected to gold coating prior to SEM imaging.

The nitrogen adsorption/desorption isotherms at 77 K were measured in an automated volumetric system (AUTOSORB-1, Quantachrome Instruments). Prior to measurement, the samples were outgassed at 250 °C for 12 h.

The infrared spectra (IR) spectra were obtained using a Thermo Scientific Nicolet 6700 FTIR equipped with a N₂ purging system and a LN₂-cooled wide range Mercuric Cadmium Telluride detector.

2.4. Adsorption kinetic analysis

Four different kinetic models (pseudo-first order, pseudo-second order, Elovich equation and intraparticle diffusion model) were used to investigate the mechanism of adsorption experiments in batch operations (Doğan *et al.*, 2007).

The pseudo-first-order kinetic model is given by the following equation:

$$\log(X_e - X_t) = \log X_e - \frac{k_1}{2.303} t \quad (1)$$

where X_e and X_t are the amounts, of dye adsorbed per unit mass of adsorbent at equilibrium and at time t, respectively and k₁ is the equilibrium rate constant (μmolg⁻¹min⁻¹). The slope of the plot of log(X_e-X_t) versus t was used to determine k₁ (μmolg⁻¹ min⁻¹) and the intercept X_e.

The pseudo – second order kinetic model can be expressed as follows:

$$\frac{t}{X_t} = \frac{1}{k_2 X_e^2} + \frac{t}{X_e} \quad (2)$$

where k₂ (μmolg⁻¹min⁻¹) is the equilibrium rate constant of pseudo-second-order adsorption. The slope of the plot of t/q_t versus t was used to determine X_e; k₂ was calculated from the intercept.

Elovich equation was established through the work of Zeldowitsch dealing with the adsorption of carbon monoxide on manganese dioxide (Zeldowitsch, 1934):

$$X_t = (1/\beta) \ln(\alpha\beta) + (1/\beta) \ln t \quad (3)$$

In this case the slope of the straight line obtained by plotting X_t versus ln t, is used to determine 1/β, and then from the intercept, the adsorption quantity, ln(αβ)/β is calculated.

Adsorption kinetics is usually controlled by diffusion (Srihari and Das, 2008). The intraparticle diffusion model can be defined as:

$$X_t = k_i t^{0.5} + C \quad (4)$$

where X_t is the amount adsorbed at time t , and k_i ($\mu\text{mol g}^{-1} \text{min}^{-0.5}$) is the intraparticle diffusion rate constant (C is the intercept). If the regression of X_t versus $t^{0.5}$ is linear and passes through the origin, then intraparticle diffusion is the sole rate-limiting step. Otherwise other mechanisms take place along with intraparticle diffusion.

2.5. MB adsorption isotherms

The equilibrium adsorption data were analysed on the basis of the Langmuir and Freundlich isotherms.

The Langmuir equation is, probably, the best known and most widely applied adsorption isotherm. This model assumes that adsorption takes place at a specific adsorption site. Langmuir isotherm is expressed as follows:

$$X_e = \frac{X_m k_L C_e}{1 + k_L C_e} \text{ or } \frac{C_e}{X_e} = \frac{1}{k_L X_m} + \frac{1}{X_m} C_e \quad (5)$$

where X_e is the amount of MB adsorbed per unit mass of adsorbent in equilibrium ($\mu\text{mol g}^{-1}$), C_e is the equilibrium MB concentration in the solution ($\mu\text{mol L}^{-1}$), X_m is the amount of solute adsorbed per unit mass of adsorbent when a complete monolayer is formed on the surface (monolayer capacity), and k_L is the Langmuir adsorption equilibrium constant related to the adsorption's energy (Alkan *et al.*, 2004). Large k_L values indicate the higher affinity of adsorbent to adsorbate.

Freundlich's empirical equation for the description of adsorption processes is based on the assumption that the surface of the adsorbent is heterogeneous and comprises of energetically different classes of adsorption sites. Adsorption on each of these sites follows the Langmuir isotherm. One of the main assumptions is that the sorbent is not saturated by the sorbate; as such infinite surface coverage is predicted, indicating multilayer sorption on the surface. Freundlich equation can be described by:

$$X_e = k_F C_e^n \text{ or } \log X_e = \log k_F + n \log C_e \quad (6)$$

where C_e ($\mu\text{mol L}^{-1}$) is the equilibrium concentration of MB (Kumar and Sivanesan, 2006). The parameters k_F and n can be derived from the respective linear plot.

3. Results & discussion

3.1. Characterization of adsorbent

The wide-angle XRD pattern of the calcined binary mesoporous ($\text{SiO}_2\text{-CaO}$) material depicted in Figure 2b confirms the amorphous nature of the material as it has been seen in similar materials (Baikousi *et al.*, 2008). In the low angle region the powder XRD pattern shows a strong peak at $2\theta = \text{ca. } 1.7$ suggesting the well ordered arrangement of the respective mesopores (Yang *et al.*, 2014; Arcos *et al.*, 2011; Bairo *et al.*, 2012).

The SEM images (see Figure 2b) show porous spherical-like aggregated ceramic spheres with diameter between 300–400 nm.

The N_2 adsorption/desorption isotherm at 77 K of the calcined binary ceramic material is presented in Figure 3a. It exhibits a typical type IV isotherm with hysteresis, characteristic for mesoporous materials. The analysis of the respective data showed a BET specific surface area of $134 \text{ m}^2/\text{g}$, total pore volume of $0.169 \text{ cm}^3/\text{g}$ and a mean pore size ca. 4.8 nm, as seen in the inset of Figure 3a. According to literature (Liang *et al.*, 2013), PEG may act as a pore-forming agent because of its thermal decomposition in this new synthetic approach. The resulting binary ceramic system can be directly transformed after a calcination process into an ordered mesoporous structure.

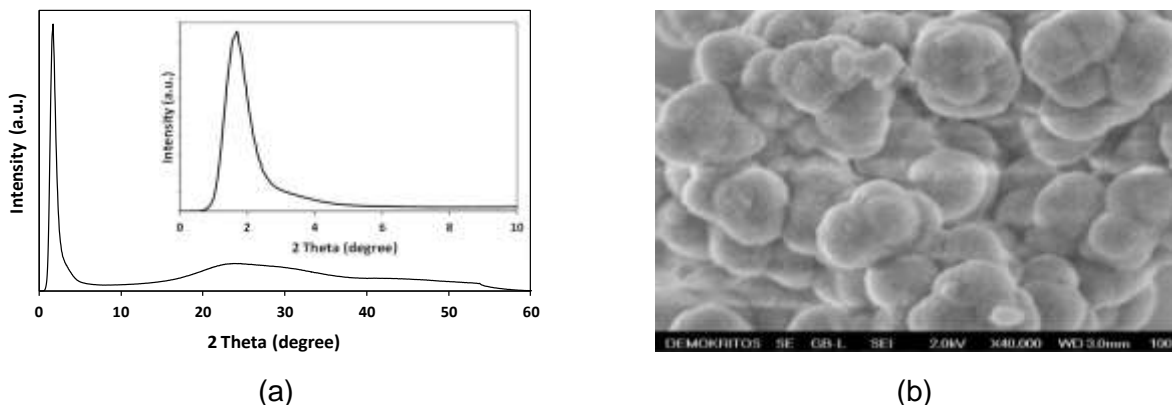


Figure 2: (a) Wide-angle XRD pattern and (b) Representative SEM image of calcined binary ceramic material.

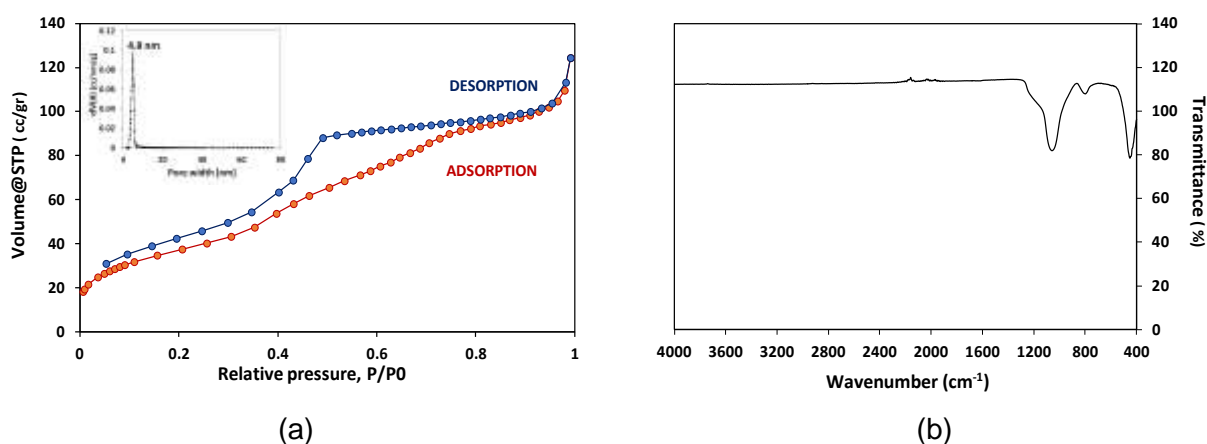


Figure 3: (a) N₂ adsorption/desorption isotherms and the corresponding pore size distribution curve (inset) of the sample after calcination at 600 °C for 5h, (b) Infrared spectrum of the sample after calcination at 600 °C for 5h.

FTIR pattern of the sample after calcination at 600 °C (see Figure 3b), depicts 3 peaks at 452 cm⁻¹, 798 cm⁻¹ and 1059 cm⁻¹, respectively. The peak at 452 cm⁻¹ is assigned to the bending modes of the Si-O-Si and O-Si-O bonds (Deb *et al.*, 2005; Kokubo *et al.*, 1990). The peak at 798 cm⁻¹ corresponds to the stretching mode of the O-Si-O bond (Deb *et al.*, 2005; Kokubo *et al.*, 1990; Vallet-Regi *et al.*, 2003). The peak at 1059 cm⁻¹ is attributed to the symmetric stretching vibration of the Si-O-Si bonds (Deb *et al.*, 2005; Vallet-Regi *et al.*, 2003). The vibration of H₂O (vibration due to the OH bond) is at 1626 cm⁻¹ (Deb *et al.*, 2005; Kokubo *et al.*, 1990; Vallet-Regi *et al.*, 2003). No peaks assigned to organic matter have been observed.

3.2. Adsorption kinetic data

The kinetic data as recorded from the adsorption experiments at 23.5°C (Figure 4a), showed the maximum amount of MB adsorption per g of adsorbent, which was equal to 65.52 μmol g⁻¹ at 28 min. The lowest MB adsorption was equal to 10.34 μmol g⁻¹ at 59 min. According to Figure 4b the highest percentage of MB adsorption (97.83% at 25 min) was presented at a ratio of adsorbent to solution equal to 3 g L⁻¹ while the lowest percentage of MB adsorption (5.04% at 59 min) was presented at a ratio of adsorbent to solution equal to 0.5 g L⁻¹. Comparing MB adsorption percentage onto SiO₂-CaO at two different ratio 3.0 and 1.5 g/L, it can be seen that the adsorption percentage for the first ratio was high enough from the first 5 min (93.90 %) compared to the adsorption percentage of the second ratio (less than 80%). As such the percentage of MB adsorption from aqueous solutions onto the binary ceramic adsorbent increases with the increase of the adsorbent to adsorbate solution ratio.

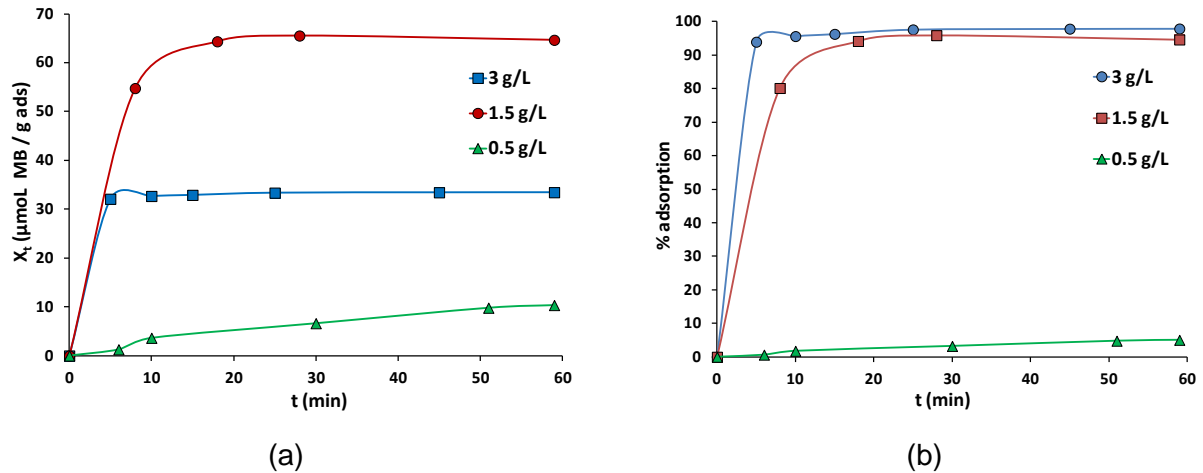


Figure 4: (a) Adsorption of MB per gram of adsorbent and (b) adsorption percentage of MB dye from aqueous solutions onto the binary ceramic system for three ratios of adsorbent to adsorbate solution, i.e. 0.5, 1.5, 3.0 g L⁻¹

The analysis of MB adsorption data in equilibrium allowed the calculation of either experimental ($X_{e,exp.}$) or theoretical ($X_{e,theor.}$) and correlation coefficient factor (r^2) values applied to all kinetic models (Table 1a). The pseudo-second order kinetic model fitted well the experimental MB adsorption data onto SiO₂-CaO for adsorbent to adsorbate solution ratio equal to 1.5 and 3.0 g L⁻¹, in agreement with other studies involving MB adsorption by activated carbons (Wang *et al.*, 2015), while the pseudo-first order was shown to be more suitable for the case of the adsorbent to adsorbate solution ratio 0.5 g L⁻¹. Intraparticle diffusion model and Elovich equations presented relatively low r^2 values showing their inappropriateness for analyzing the experimental data of the entire adsorption process. The application of the pseudo-second order model has shown that the increase of adsorbent to adsorbate solution ratio led to an increase in the equilibrium rate constant, k_2 .

Table 1: (a) Kinetic and (b) equilibrium parameters for the adsorption of MB onto SiO₂-CaO

where $X_{e,exp}$ and $X_{e,theor.}$ units are $\mu\text{mol dye}\cdot\text{g}^{-1}\text{ ads.}$, k_1 and k_2 units are $\mu\text{mol dye}\cdot\text{g}^{-1}\text{ ads.}\cdot\text{min}^{-1}$, $\ln(\alpha\beta)/\beta$

Adsorbent to solution ratio (g L ⁻¹)	$X_{e, exp.}$	Pseudo-first order			Pseudo-second order			Elovich equation			Intraparticle diffusion	
		k_1	$X_{e, theor.}$	R^2	k_2	$X_{e, theor.}$	R^2	α	β	R^2	k_i	R^2
0.5	165.65	$8.47\cdot 10^{-4}$	163.54	0.99	$3.38\cdot 10^{-6}$	253.64	0.76	1.62	0.04	0.80	4.12	0.94
1.5	64.65	0.30	77.93	0.99	0.02	66.00	0.99	$7.07\cdot 10^4$	0.20	0.66	8.33	0.71
3.0	33.44	0.15	6.46	0.87	0.12	33.60	1.00	$2.29\cdot 10^{24}$	1.81	0.93	3.36	0.50

and $1/\beta$ units are $\mu\text{mol g}^{-1}\text{ ads.}$ and $\mu\text{mol}\cdot\text{min g}^{-1}\text{ ads.}$, k_i units are $\mu\text{mol dye}\cdot\text{g}^{-1}\text{ ads.}\cdot\text{min}^{-0.5}$

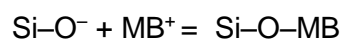
(a)

Langmuir			Freundlich		
k_L	X_m	R^2	n	k_F	R^2
0.04	357.14	0.96	0.74	18.61	1.00

where X_m units are $\mu\text{mol dye}\cdot\text{g}^{-1}\text{ ads.}$, k_L and k_F units are min^{-1} and $\text{g}\cdot\mu\text{mol}^{-1}\text{min}^{-1}$

(b)

According to Figure 5a, it seems that pH ranges from 7.7 to 8.7 in relation to the adsorbent to solution ratio at 23.5°C. The high solution pH is a crucial factor indicating the presence of -Si-O- groups which has relatively strong electrostatic or chemical association with MB facilitating the adsorption of positively charged adsorbates onto the negatively charged adsorbent (Chen *et al.*, 2007; Ho, 2006). The pH-dependent adsorption of MB onto SiO₂-CaO may be described as follows:



According to literature (Elmorsi, 2011), anionic dyes are favorably adsorbed by the adsorbent at low pH values due to the presence of H⁺ ions while adsorption of cationic dyes such as methylene blue are favorably adsorbed at high pH values, which led to increase the presence of

OH^- ions as a result of an increase to the electrostatic attraction. Consequently, the basic solution pH increases the negative charge on the adsorbent surface leading to an increase in the electrostatic attraction between cationic dye molecules, e.g. methylene blue and the $\text{SiO}_2\text{-CaO}$ surface. Thus, the adsorption capacity is affected by the electrostatic interaction and chemical association of the functional groups, i.e. $-\text{Si-O}^-$.

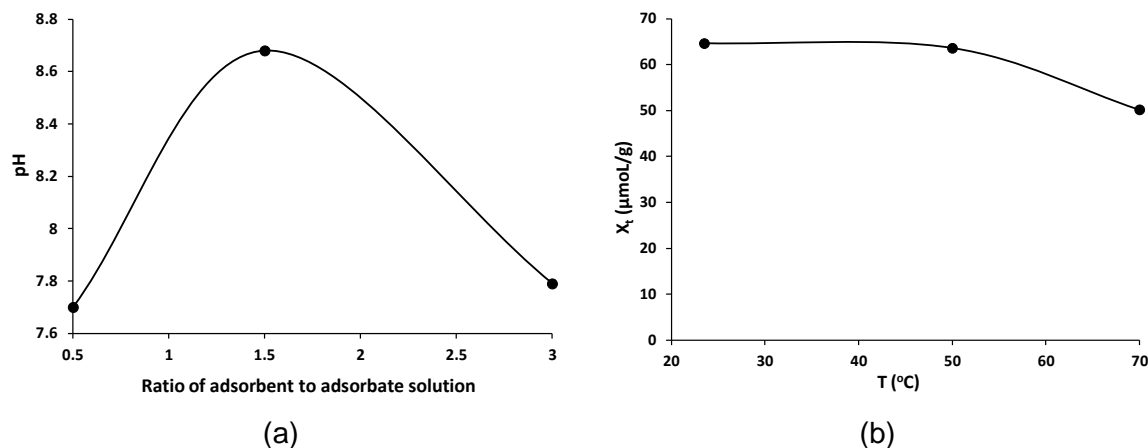


Figure 5: (a) pH range, during the adsorption of MB onto $\text{SiO}_2\text{-CaO}$ for different ratios of adsorbent to adsorbate solution, i.e. 0.5, 1.5, 3 g L^{-1} and (b) influence of temperature, i.e. 24, 50, 70 $^\circ\text{C}$ for adsorbent to adsorbate solution ratio equal to 1.5 g L^{-1}

Examining the dependence of temperature to MB adsorption onto $\text{SiO}_2\text{-CaO}$ (Fig. 6b), it seems that MB adsorption in equilibrium presented values between 50.20 and 64.65 $\mu\text{mol g}^{-1}$ for temperatures between 23.5 and 70 $^\circ\text{C}$. This implies that temperature affects only slightly MB adsorption from aqueous solutions onto $\text{SiO}_2\text{-CaO}$ showing that the adsorption process depends primarily on the interaction of MB with the functional groups of $\text{SiO}_2\text{-CaO}$. Moreover, the increase of temperature beyond 50 $^\circ\text{C}$ led to the decrease of MB adsorption in equilibrium indicating probably a slight desorption of MB at higher temperatures. According to literature (Luo *et al.*, 2015) an increase in temperature can favour the transfer and diffusion of the adsorbate from the bulk solution to the adsorbent's surface due to the lower viscosity of the solution. It has also been reported that the increase in temperature has as a result an increase in the mobility of the adsorbate molecules previously adsorbed (Doğan *et al.*, 2000).

3.3 Equilibrium adsorption data

At constant methylene blue (MB) concentration (0.0328 g L^{-1}) different amounts of $\text{SiO}_2\text{-CaO}$ were added to MB solution, i.e. 0.5, 1.0, 1.5, 3.0 g L^{-1} (see Figure 6) at 23.5 $^\circ\text{C}$. The results show that MB concentration in the solution increased rapidly with the decrease in the adsorbent dose. It can be seen that at 3.0 g L^{-1} of the adsorbent dose, the adsorption MB capacity reached 33.44 $\mu\text{mol g}^{-1}$ and MB concentration in the solution reached 2.22 $\mu\text{mol L}^{-1}$. Then a decrease in the dose of $\text{SiO}_2\text{-CaO}$ from 3.0 to 0.5 g L^{-1} led to an adsorption MB capacity equal to 165.65 $\mu\text{mol g}^{-1}$ and MB concentration in the solution at 19.72 $\mu\text{mol L}^{-1}$. The decrease in MB solution in equilibrium with the increase in adsorbent dose can be assigned to the increase in the adsorption sites of $\text{SiO}_2\text{-CaO}$ to MB dye molecules. Other studies have shown similar results (Hameed *et al.*, 2007; Hameed, 2009; Uma *et al.*, 2009).

The experimental MB adsorption data were analysed using Langmuir and Freundlich isotherms (Table 1b). The applicability of these equations was quantitatively assessed by the correlation coefficient factor (r^2). It was found that Freundlich isotherm, which assumes multilayer adsorption, is more suitable for the description of MB adsorption data onto $\text{SiO}_2\text{-CaO}$. On the other hand, Langmuir isotherm, which assumes monolayer adsorption, cannot fit well the experimental adsorption data. According to Table 1b, the values of n are lower than unity

indicating the degree of surface heterogeneity and reflecting the favorable adsorption of the dye over the entire concentration range used in this study ($0.5\text{-}3\text{ g L}^{-1}$) (Al-Degs *et al.*, 2008).

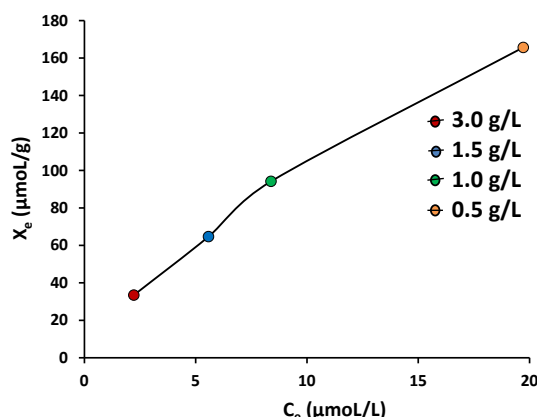


Figure 6: Equilibrium study of MB adsorption onto $\text{SiO}_2\text{-CaO}$ for different ratios of adsorbent to adsorbate solution, i.e. 0.5, 1.0, 1.5, 3.0 g L^{-1} .

4. Conclusions

An ordered mesoporous binary ceramic material ($\text{SiO}_2\text{-CaO}$) has been successfully synthesized by a hydrothermal method and proved to be an efficient adsorbent for methylene blue removal from aqueous solutions. The XRD analysis confirms the amorphous well-ordered mesoporous structure of the material, which comprises of aggregated spheres. The MB adsorption capacity of the new material is affected by the electrostatic interaction and chemical association of the functional groups, i.e. $-\text{Si-O}^-$. The adsorption equilibrium data were best described by the Freundlich isotherm, giving a maximum sorption capacity equal to $165.65\ \mu\text{mol g}^{-1}$ at $23.5\ ^\circ\text{C}$.

ACKNOWLEDGMENTS

D. Baciú gratefully acknowledges Mr. G. Pilatos, Ms. L. Boutsika, Ms. D. Giasafaki and Mr. C. Tampaxis, HYSORB Lab, Institute of Nanoscience and Nanotechnology National Center for Scientific Research "Demokritos", for their kind help for SEM, XRD and porosimetry measurements.

REFERENCES

1. Al-Degs Y. S., El-Barghouthi M. I., El-Sheikh A. H., Walker G. M. (2008), Effect of solution pH, ionic strength and temperature on adsorption behavior of reactive dyes on activated carbon, *Dyes and Pigments*, **77**, 16-23.
2. Alkan M., Demirbaş Ö., Çelikçapa S., Doğan M. (2004), Sorption of Acid Red 57 from aqueous solution onto sepiolite. *J. Hazard. Mater.* **B116**, 135–145.
3. Arcos D., Vila M., López-Noriega A., Rossignol F., Champion E., Oliveira F.J., Vallet-Regí M., (2011), Mesoporous bioactive glasses: Mechanical reinforcement by means of a biomimetic process, *Acta Biomaterialia* **7**, 2952–2959.
4. Baikousi M., Agathopoulos S., Panagiotopoulos I., Georgoulis A. D., Louludi M., Karakassides M. A. (2008), Synthesis and characterization of sol-gel derived bioactive $\text{CaO-SiO}_2\text{-P}_2\text{O}_5$ glasses containing magnetic nanoparticles, *J Sol-Gel Sci Technol*, **47**,95–101.
5. Bairo F., Fiorilli S., Mortera R., Onida B., Saino E., Visai L., Verné E., Vitale-Brovarone C. (2012), Mesoporous bioactive glass as a multifunctional system for bone regeneration and controlled drug release, *Journal of Applied biomaterials & functional materials*, **10**, 12-21.
6. Chen H., Zhao Y.G., Wang A.Q. (2007), Removal of Cu(II) from aqueous solutions by adsorption onto acid-activated palygorskite, *J. Hazard. Mater.* **149**, 346-354.
7. Deb S., Aiyathurai L., Roether J. A., Luklinska Z. B. (2005), Development of high viscosity two paste bioactive bone cements, *Biomaterials* **26**, 3713-3718.
8. Doğan M., Alkan M., Onganer Y., (2000), Adsorption of methylene blue from aqueous solutions onto perlite, *Water Air Soil Pollut.*, **120**, 229-248.

9. Doğan M., Özdemir Y., Alkan M. (2007), Adsorption kinetics and mechanism of cationic methyl violet and methylene blue dyes onto sepiolite, *Dyes and Pigments*, **75**, 701-713.
10. Elmorsi T. M. (2011), Equilibrium isotherms and kinetic studies of removal of methylene blue dye by adsorption onto Miskwak leaves as a natural adsorbent, *Journal of Environmental Protection*, **2**, 817-827.
11. Fu J., Chen Z., Wang M., Liu S., Zhang J., Zhang J., Han R., Xu Q. (2015), Adsorption of methylene blue by a high-efficiency adsorbent (polydopamine microspheres): Kinetics, isotherm, thermodynamics and mechanism analysis, *Chemical Engineering Journal* **259**, 53–61.
12. Ghaedia M., A Golestani. N., Khodadoust S., Sahraei R., Daneshfar A. (2015), Characterization of zinc oxide nanorods loaded on activated carbon as cheap and efficient adsorbent for removal of methylene blue, *Journal of Industrial and Engineering Chemistry* **21**, 986–993
13. Hameed B. H., Din A. T. M. and Ahmad A. L. (2007), Adsorption of methylene blue onto bamboo-based activated carbon: Kinetics and equilibrium studies, *J. Hazard. Mater.* **141(3)**, 819-825.
14. Hameed B. H. (2009), Grass waste: A novel sorbent for the removal of basic dye from aqueous solution, *J. Hazard. Mater.* **166 (1)**, 233-238.
15. Ho Y.-S. (2006), Review of second order models for adsorption systems, *J. Hazard. Mater.* **B136**, 681-689.
16. Kokubo T., Kushitani H., Sukka S., Kitsugi T., Yamamuro T. (1990), Solutions able to reproduce in vivo surface-structure changes in bioactive glass-ceramic A-W, *J. Biomed. Res.* **24**, 721-734.
17. Kumar K. V., Sivanesan S. (2006), Equilibrium data, isotherm parameters and process design for partial and complete isotherm of methylene blue onto activated carbon, *J. Hazard. Mater.*, **B134**, 237–244
18. Liang Y. , Lu S. , Wu D. , Sun B. , Xu F. and Fu R. (2013), Polyethylene glycol-induced self-assembly to synthesize an ordered mesoporous polymer with a two-dimensional hexagonal structure, *Mater. Chem. A*, **1**, 3061-3067.
19. Luo D., Yu Q. W., Yin H. R., Feng Y. Q. (2007) Humic acid-bonded silica as a novel sorbent for solid-phase extraction of benzo[a]pyrene in edible oils., *Anal. Chim. Acta.* **588**, 261-267.
20. Salonen, J.; Laitinen, L.; Kaukonen, A. M.; Tuura, J.; Bjorkqvist, M.; Heikkila, T.; Vaha-Heikkila, K.; Hirvonen, J.; Lehto, V. P.J.,(2005), Mesoporous silicon microparticles for oral drug delivery: loading and release of five model drugs, *Controlled Release* **108 (2)**, 362 -374.
21. Srihari V., Das A. (2008), The kinetic and thermodynamic studies of phenol-sorption onto three agro-based carbons, *Desalination* **225**, 220-234.
22. Uma R. L., Srivastava V. C., Mall I. D., Lataye D. H. (2009), Rice husk ash as an effective adsorbent: Evaluation of adsorptive characteristics for Indigo Carmine dye, *J. Environ. Management* **90 (2)**, 710-720.
23. Vallet-Regi M., Ragel C. V., Salinas A. (2003), Glasses with Medical Applications, *Eur. J. Inorg. Chem.*, 1029-1042.
24. Vallet-Regi, M.; Izquierdo-Barba, I.; Ramila, A.; Perez-Pariente, J.; Babonneau, F.; Gonzalez-Calbet, (2005), Phosphorous doped MCM-41 as bioactive material, *J. M.Solid State Sci.* **7**, 233-237.
25. Xiao X., Zhang F., Feng Z., Deng S., Wang Y. (2015), Adsorptive removal and kinetics of methylene blue from aqueous solution using NiO/MCM-41 composite, *Physica* **E 65**, 4–12.
26. Zarezadeh-Mehrzi M., Badieli A. (2014), Highly efficient removal of basic blue 41 with nanoporous silica, *Water Resources and Industry* **5**, 49–57.
27. Zeldowitsch J. (1934), Über den mechanismus der katalytischen oxydation von CO an MnO₂, *Acta Physicochimica URSS*, **1**, 364-449.
28. Zhao X.S., Lu G.Q., Millar G.J. (1996), Advances in mesoporous molecular sieve MCM-41, *Ind. Eng. Chem. Res.* **35**, 2075–2090.
29. Yan, X. X.; Deng, H. X.; Huang, X. H.; Lu, G. Q.; Qiao, S. Z.; Zhao, D. Y.; Yu, C. Z.J. (2005), Mesoporous bioactive glasses. I. Synthesis and structural characterization, *Non-Cryst. Solids*, **351**, 3209-3217.
30. Yang, Q.; Wang, S. H.; Fan, P. W.; Wang, L. F.; Di, Y.; Lin, K. F.; Xiao, F-S. (2005), *Chem. Mater.*, **17**, 5999-6003.
31. Yang C., Guo W., Cui L., Xiang D., Cai K., Lin H., Qu F., (2014), pH-responsive controlled-release system based on mesoporous bioglass materials capped with mineralized hydroxyapatite, *Materials Science and Engineering* **C 36**, 237–243.
32. Wang W., G. Tian, Zhang Z., Wang A. (2015), A simple hydrothermal approach to modify palygorskite for high-efficient adsorption of Methylene blue and Cu(II) ions, *Chemical Engineering Journal*, **265**, 228-238.